

Jagiellonian University in Krakow

Faculty of Physics, Astronomy
and Applied Computer Science



Piotr Sierant

Path integral approach to a simple quantum mechanical system

bachelor thesis written under supervision
of Prof. Jacek Wosiek

Krakow, 2013

Contents

1. Introduction	2
2. The path integral	3
2.1. Feynman’s kernel	3
2.2. The Wick rotation	4
2.3. Averages of physical quantities	4
2.4. The point-splitting prescription	7
3. Numerical evaluation of path integrals	9
3.1. Calculating path integrals using Monte Carlo methods	9
3.2. The Metropolis algorithm	10
3.3. Estimation of statistical errors	11
4. Results for harmonic oscillator	13
4.1. Units and scales of the problem	13
4.2. Thermalization, autocorrelation and critical slowing down	13
4.3. Fundamental observables \hat{x}^2, \hat{p}^2	16
4.4. The ground state of the system	17
4.5. Two-point correlation functions	19
4.5.1. Definition and relation to the higher energy states	19
4.5.2. The first excited state of the harmonic oscillator	20
4.5.3. The second excited state	21
5. Summary	23
Acknowledgements	24
References	25

1. Introduction

The path integral formulation of quantum mechanics was developed in 1948 by Richard Feynman and played a crucial role in progress of theoretical physics. The path integral approach to quantum mechanics, presented in details in book [1] by R.Feynman and A.Hibbs, reveals connection between the elegant Lagrange approach to classical mechanics and the quantum mechanics. Furthermore, it provides intuitive insights into behavior of quantum mechanical system for it shows that the matrix element of evolution operator can be calculated as sum over all trajectories connecting the starting and final state of the system.

Numerical computation of path integrals in imaginary time formalism with use of Monte Carlo techniques proved to be an efficient way of solving non-perturbative quantum problems, led to development of the lattice field theory and become a powerful tool in investigation of QCD.

In this thesis we employ the numerical method to evaluate path integrals in a simple context of one dimensional quantum mechanics, which already exhibits properties that are encountered in study of more advanced theories.

M. Creutz and B. Freedman considered anharmonic oscillator in [3] in a similar fashion. In [6] a study of three different Monte Carlo algorithms is presented.

Plan of the thesis is the following. We start with a brief introduction of the path integral formalism, perform transition to Euclidean time in section 2. Moreover, relationships between operators and functionals, essential in our considerations are examined and derived. In section 3 we present the numerical method of evaluating the path integrals. Then, in section 4, the presented technique is applied to the case of harmonic oscillator.

2. The path integral

2.1. Feynman's kernel

A wave function of a single one dimensional non-relativistic quantum particle subjected to the potential $V(x)$ is a solution of the Schrödinger equation:

$$i\hbar \frac{\partial}{\partial t} \psi(x, t) = \hat{H} \psi(x, t) \quad (2.1)$$

where the Hamiltonian $\hat{H} = \frac{\hat{p}^2}{2m} + V(\hat{x})$. If at time $t = t_a$ the wave function is $\psi(x_a, t_a)$, then at time $t_b > t_a$ it is given by:

$$\psi(x_b, t_b) = \int_{-\infty}^{\infty} dx K(x_b, t_b; x, t_a) \psi(x, t_a), \quad (2.2)$$

where the kernel function $K(x_b, t_b; x_a, t_a)$ can be calculated as the Feynman's renowned path integral:

$$K(x_b, t_b; x_a, t_a) = \int_{x_b \leftarrow x_a} \mathcal{D}x(t) \exp \left(\frac{i}{\hbar} S[x(t)] \right) = \int_{x_b \leftarrow x_a} \mathcal{D}x(t) \exp \left(\frac{i}{\hbar} \left(\frac{m}{2} \dot{x}(t)^2 - V(x(t)) \right) \right), \quad (2.3)$$

the action $S[x(t)]$ is computed for a trajectory $x(t)$ connecting points (x_a, t_a) and (x_b, t_b) .

The path integral (2.3) is constructed as follows:

- the time interval $[t_a, t_b]$ is split into N_T steps of length ε and the beginning of each time step is denoted as t_i ($i = 0, 1, \dots, N_T$),
- a position x_i is associated with each time t_i and points (x_i, t_i) , (x_{i+1}, t_{i+1}) are connected with straight lines. Provided that $x_0 = x_a$ and $x_{N_T} = x_b$, a discretized trajectory $x_{N_T}(t)$, which connects points (x_a, t_a) and (x_b, t_b) , is defined in this way.
- the value of action is computed for the trajectory obtained from the procedure of time discretization:

$$S[x_{N_T}(t)] = \int_{t_a}^{t_b} dt \left(\frac{m}{2} \dot{x}(t)^2 - V(x(t)) \right) = \sum_{j=0}^{N_T-1} \varepsilon \left(\frac{m}{2} \left(\frac{x_{j+1} - x_j}{\varepsilon} \right)^2 - V(x_j) \right) + O(\varepsilon^2) \quad (2.4)$$

and one claims that the propagator for the trajectory is given by:

$$K_{N_T}(x_b, t_b; x_a, t_a) = \left(\frac{m}{2\pi i \hbar \varepsilon} \right)^{\frac{N_T-1}{2}} \int_{x_b \leftarrow x_a} \prod_{j=1}^{N_T-1} dx_j \exp \left(\frac{i}{\hbar} S[x_{N_T}(t)] \right) \equiv \int_{x_b \leftarrow x_a} \mathcal{D}x_{N_T}(t) \exp \left(\frac{i}{\hbar} S[x_{N_T}(t)] \right) \quad (2.5)$$

- in the limit $N_T \rightarrow \infty$, which we refer to as the continuum limit, the discrete time trajectories can approximate any physical trajectory $x(t)$ connecting points (x_a, t_a) and (x_b, t_b) , thus the path integral is defined as the following limit:

$$\int_{x_b \leftarrow x_a} \mathcal{D}x(t) \exp \left(\frac{i}{\hbar} S[x(t)] \right) = \lim_{N_T \rightarrow \infty} \int_{x_b \leftarrow x_a} \mathcal{D}x_{N_T}(t) \exp \left(\frac{i}{\hbar} S[x_{N_T}(t)] \right). \quad (2.6)$$

The integration in (2.5) is carried out over all intermediate points x_1, \dots, x_{N_T-1} , consequently the path integral can be interpreted as a sum over all paths connecting the points (x_a, t_a) and (x_b, t_b) .

2.2. The Wick rotation

The Wick rotation is a procedure of transition to imaginary time and proves to be essential in numerical calculations of path integrals. The Euclidean time is introduced as:

$$\tau = it, \quad (2.7)$$

using the above equation in the definition of action one finds:

$$S[x(t)] = \int_{t_a}^{t_b} dt \left(\frac{m}{2} \left(\frac{dx}{dt} \right)^2 - V(x(t)) \right) = i \int_{\tau_a}^{\tau_b} d\tau \left(\frac{m}{2} \left(\frac{dx}{d\tau} \right)^2 + V(x(\tau)) \right) \equiv iS_E[x(t)], \quad (2.8)$$

the last equality defines the Euclidean action S_E .

Real values of τ will be considered, which means that we will be dealing with the evolution of a quantum system for imaginary values of time t .

The exponent $e^{\frac{i}{\hbar}S[x(t)]}$ - a complex-valued and oscillatory function of $S[x(t)]$ becomes $e^{-\frac{1}{\hbar}S_E[x(t)]}$ - a real-valued and exponentially damped function, which is a desired feature in numerical computations.

Another implication of the transition to imaginary time is the fact, that the evolution of a quantum system is no longer unitary. Denoting by $|n\rangle$ the n -th eigenstate of the Hamiltonian \hat{H} , i.e. $\hat{H}|n\rangle = E_n|n\rangle$ ($E_{n+1} > E_n$) and assuming that the system has discrete energy spectrum, we find:

$$|\psi(\tau_b)\rangle = e^{-\frac{1}{\hbar}\hat{H}(\tau_b-\tau_a)}|\psi(\tau_a)\rangle = e^{-\frac{1}{\hbar}\hat{H}(\tau_b-\tau_a)} \sum_{i=0}^{\infty} c_i |i\rangle = \sum_{i=0}^{\infty} e^{-\frac{1}{\hbar}E_i(\tau_b-\tau_a)} c_i |i\rangle, \quad (2.9)$$

where E_n is the energy of the state $|n\rangle$. Unless the state $|\psi\rangle$ is orthogonal to $|0\rangle$, it is projected to vacuum for $\tau_b \rightarrow +\infty$.

In order to simplify notation we will denote the Euclidean time by t and the Euclidean action by S in the rest of this paper.

2.3. Averages of physical quantities

Our purpose is to evaluate path integrals numerically, we therefore restrict ourselves to the discrete time trajectories $x_{N_T}(t)$, since limit $N_T \rightarrow \infty$ cannot be performed on a computer. We intend to extract physically meaningful information about a quantum system, thus a need to consider operators representing physical quantities in quantum mechanics, which are related to functionals evaluated for discretized paths $x_{N_T}(t)$, arises.

Let us define the partition function as:

$$Z_{N_T} \equiv \int dx \int_{x \leftarrow x} \mathcal{D}x_{N_T}(t) \exp \left(-\frac{1}{\hbar} S[x_{N_T}(t)] \right) \equiv \int \mathcal{D}x_{N_T}(t) \exp \left(-\frac{1}{\hbar} S[x_{N_T}(t)] \right), \quad (2.10)$$

the integration is carried over paths connecting points $(x, t=0)$, $(x, t=T)$ and the result is integrated over x , the last equality in (2.10) simplifies the notation.

The partition function (2.10) is related to the evolution operator $\hat{U}(T, 0) = e^{-\hat{H}T}$ known from the Schrödinger formulation of quantum mechanics in an interesting way, which will be now shown. The first step is to note that the action $S[x_{N_T}(t)]$ can be written as a sum of terms depending only on the values of variables on the neighboring time slices:

$$Z_{N_T} = \int \mathcal{D}x_{N_T}(t) \exp \left(-\frac{1}{\hbar} \sum_{i=0}^{N-1} S(x_{i+1}, x_i) \right) = \int \mathcal{D}x_{N_T}(t) \prod_{i=0}^{N_T-1} \exp \left(-\frac{1}{\hbar} S(x_{i+1}, x_i) \right), \quad (2.11)$$

where

$$S(x_{i+1}, x_i) = \frac{m}{2\varepsilon}(x_{i+1} - x_i)^2 + \frac{\varepsilon}{2}V(x_{i+1}) + \frac{\varepsilon}{2}V(x_i) + \mathcal{O}(\varepsilon^2). \quad (2.12)$$

We now assume that there exists an operator on the Hilbert space of states $\hat{\mathcal{T}} : \mathcal{H} \rightarrow \mathcal{H}$ such that the matrix element of $\hat{\mathcal{T}}$ between eigenstates of the position operator \hat{x} (i.e. $\hat{x}|x\rangle = x|x\rangle$) reads:

$$\langle x|\hat{\mathcal{T}}|x'\rangle = \sqrt{\frac{m}{2\pi\hbar\varepsilon}} \exp\left(-\frac{1}{\hbar}S(x, x')\right). \quad (2.13)$$

The matrix (2.13) is known as the transfer matrix. Employing the momentum operator \hat{p} as a generator of translations, equation (2.13) can be rewritten as:

$$\langle x|\hat{\mathcal{T}}|x'\rangle = \sqrt{\frac{m}{2\pi\hbar\varepsilon}} \int_{-\infty}^{\infty} d\Delta e^{-\frac{\varepsilon}{2\hbar}V(x)} e^{-\frac{\Delta^2}{2\varepsilon\hbar}m} \langle x|e^{-\frac{i}{\hbar}\hat{p}\Delta}|x'\rangle e^{-\frac{\varepsilon}{2\hbar}V(x')} \quad (2.14)$$

However, the last equation means that $\hat{\mathcal{T}}$ can be expressed as a function of the momentum and position operators:

$$\hat{\mathcal{T}} = \sqrt{\frac{m}{2\pi\hbar\varepsilon}} e^{-\frac{\varepsilon}{2\hbar}V(\hat{x})} \left[\int_{-\infty}^{\infty} d\Delta e^{-\frac{\Delta^2}{2\varepsilon\hbar}m} e^{-\frac{i}{\hbar}\hat{p}\Delta} \right] e^{-\frac{\varepsilon}{2\hbar}V(\hat{x})}. \quad (2.15)$$

Calculating the gaussian integral over Δ and transforming the result with the aid of the Baker-Hausdorff formula, one finally obtains:

$$\hat{\mathcal{T}} = e^{-\frac{\varepsilon}{2\hbar}V(\hat{x})} e^{-\frac{\varepsilon}{\hbar}\frac{\hat{p}^2}{2m}} e^{-\frac{\varepsilon}{2\hbar}V(\hat{x})} = e^{-\frac{1}{\hbar}\left(\frac{\hat{p}^2}{2m} + V(\hat{x})\right)\varepsilon + \mathcal{O}(\varepsilon^2)} = e^{-\frac{1}{\hbar}\hat{H}\varepsilon + \mathcal{O}(\varepsilon^2)}. \quad (2.16)$$

Equations (2.11) and (2.13) imply that

$$Z_{N_T} = \text{Tr} \left(\hat{\mathcal{T}}^{N_T} \right), \quad (2.17)$$

moreover, using (2.16), we find the desired relationship between the evolution operator and the partition function:

$$\lim_{N_T \rightarrow \infty} Z_{N_T} = \text{Tr} \left(e^{-\frac{1}{\hbar}\hat{H}T} \right) \equiv Z_T. \quad (2.18)$$

We now proceed to define the average values of physical quantities. Let $A[x_{N_T}(t)]$ be a functional evaluated for discretized trajectories. In fact, the functional $A[x_{N_T}(t)]$ is a function of values of positions of the particle x_i at times t_i :

$$A[x_{N_T}(t)] = A(x_0, \dots, x_{N_T}), \quad (2.19)$$

since x_0, \dots, x_{N_T} specify the discretized trajectory. The average value of the functional $A[x_{N_T}(t)]$ is defined as:

$$\langle A \rangle = \frac{1}{Z_{N_T}} \int \mathcal{D}x_{N_T}(t) \exp \left(-\frac{1}{\hbar}\varepsilon \sum_{j=0}^{N-1} \left(\frac{m}{2} \frac{(x_{j+1} - x_j)^2}{\varepsilon^2} + V(x_j) \right) \right) A[x_{N_T}(t)]. \quad (2.20)$$

At this point a question about a physical quantity represented by the functional $A[x_{N_T}(t)]$ emerges. The procedure, that was carried out in order to find the relationship between the partition function and the evolution operator, can be conveniently generalized in order to find an operator formula for $\langle A \rangle$. Then, operators, which appear in the operator formula, will reveal the physical significance of $A[x_{N_T}(t)]$.

Let us consider an example of a local functional $A[x_{N_T}(t)] = f(x_k)$ where f is a smooth function (we will be particularly interested in the case of f being a polynomial). The path integral (2.20) can be decomposed as:

$$\frac{1}{Z_{N_T}} \sqrt{\frac{m}{2\pi\hbar\varepsilon}} \int \mathcal{D}x_{N_T-k}(t) dx_k \mathcal{D}x_{k-1}(t) \prod_{i=k+1}^{N_T-1} \left(e^{-\frac{1}{\hbar}S(x_{i+1},x_i)} \right) e^{-\frac{1}{\hbar}S(x_{k+1},x_k)} f(x_k) \prod_{i=0}^{k-1} \left(e^{-\frac{1}{\hbar}S(x_{i+1},x_i)} \right), \quad (2.21)$$

however, we already know how to express the integration over x, x_1, \dots, x_{k-1} and $x_{k+1}, \dots, x_{N_T-1}$ in terms of operators. Hence, one needs to perform the integration over x_k . Assuming that there exists an operator $\hat{O}_1 : \mathcal{H} \rightarrow \mathcal{H}$ which fulfills the requirement:

$$\langle x | \hat{O}_1 | x' \rangle = \sqrt{\frac{m}{2\pi\hbar\varepsilon}} \exp\left(-\frac{1}{\hbar}S(x, x')\right) f(x') \quad (2.22)$$

and repeating the steps taken in equations (2.14), (2.15) we find that:

$$\hat{O}_1 = e^{-\frac{1}{\hbar}\left(\frac{\hat{p}^2}{2m} + V(\hat{x})\right)\varepsilon + \mathcal{O}(\varepsilon^2)} f(\hat{x}). \quad (2.23)$$

Consequently, the resulting operator formula reads:

$$\langle f(x_k) \rangle = \frac{1}{Z_{N_T}} \text{Tr} \left(\hat{\mathcal{T}}^{N_T-k} f(\hat{x}) \hat{\mathcal{T}}^k \right), \quad (2.24)$$

which in the continuum limit yields

$$\langle f(x(t_k)) \rangle = \frac{1}{Z_T} \text{Tr} \left(e^{-\frac{1}{\hbar}\hat{H}(T-t_k)} f(\hat{x}) e^{-\frac{1}{\hbar}\hat{H}t_k} \right), \quad (2.25)$$

where $t_k = k\varepsilon$. Therefore, the relationship between the operators and the functionals, which depend only on one variable x_k , is straightforward. Furthermore, it is interesting to note that the trace in (2.25) is computed for the operator which is the product of $f(\hat{x})$ in time t_k (cf. Heisenberg picture of quantum mechanics) and $e^{-\frac{1}{\hbar}\hat{H}T}$, which projects to vacuum for $T \rightarrow \infty$.

The case of functionals depending on two variables x_k and x_{k+1} proves to be more complicated. We now consider a functional $p[x_{N_T}(t)] = m \frac{x_{k+1} - x_k}{\varepsilon}$, which seems to be a good candidate for a quantity related with the momentum of a particle. Decomposing the path integral as in eq. (2.21) and assuming that there exists an operator $\hat{O}_2 : \mathcal{H} \rightarrow \mathcal{H}$ whose matrix elements are

$$\langle x | \hat{O}_2 | x' \rangle = \sqrt{\frac{m}{2\pi\hbar\varepsilon}} \exp\left(-\frac{1}{\hbar}S(x, x')\right) m \frac{x' - x}{\varepsilon}, \quad (2.26)$$

we obtain the following relation

$$\hat{O}_2 = \sqrt{\frac{m}{2\pi\hbar\varepsilon}} e^{-\frac{\varepsilon}{2\hbar}V(\hat{x})} \left[\int_{-\infty}^{\infty} d\Delta \left(m \frac{\Delta}{\varepsilon} \right) e^{-\frac{\Delta^2}{2\varepsilon\hbar}m} e^{-\frac{i}{\hbar}\hat{p}\Delta} \right] e^{-\frac{\varepsilon}{2\hbar}V(\hat{x})}. \quad (2.27)$$

Substituting $\Delta' = \Delta + \frac{i\varepsilon}{\hbar}\hat{p}$ and performing the integration

$$\sqrt{\frac{m}{2\pi\hbar\varepsilon}} \int_{-\infty}^{\infty} d\Delta \left(m \frac{\Delta}{\varepsilon} \right) e^{-\frac{\Delta^2}{2\varepsilon\hbar}m} e^{-\frac{i}{\hbar}\hat{p}\Delta} = \sqrt{\frac{m}{2\pi\hbar\varepsilon}} \int_{-\infty}^{\infty} d\Delta' \left(m \frac{(\Delta' - \frac{i\varepsilon}{\hbar}\hat{p})}{\varepsilon} \right) e^{-\frac{\Delta'^2}{2\varepsilon\hbar}m} e^{-\frac{\varepsilon}{2m}\hat{p}^2} = i\hat{p} e^{-\frac{\varepsilon}{2m\hbar}\hat{p}^2}, \quad (2.28)$$

we find that the functional $p[x_{N_T}(t)]$ indeed corresponds to the momentum at time t_k , since its expectation value reads:

$$\langle p \rangle = i \frac{1}{Z_{N_T}} \text{Tr} \left(\hat{\mathcal{T}}^{N_T-k} \hat{p} \hat{\mathcal{T}}^k \right), \quad (2.29)$$

Encouraged by (2.29) one may attempt to generalize the idea and consider a functional

$$p^2[x_{N_T}(t)] = \left(m \frac{x_{k+1} - x_k}{\varepsilon} \right)^2 \quad (2.30)$$

which looks like a reasonable candidate for a quantity associated with the square of the momentum. Again, we introduce an operator \hat{O}_3 acting in the Hilbert space of states \mathcal{H} , with matrix elements given by:

$$\langle x | \hat{O}_3 | x' \rangle = \sqrt{\frac{m}{2\pi\hbar\varepsilon}} \exp \left(-\frac{1}{\hbar} S(x, x') \right) \left(m \frac{x' - x}{\varepsilon} \right)^2, \quad (2.31)$$

which, in terms of the momentum and position operators, can be expressed as

$$\hat{O}_3 = \sqrt{\frac{m}{2\pi\hbar\varepsilon}} e^{-\frac{\varepsilon}{2\hbar} V(\hat{x})} \left[\int_{-\infty}^{\infty} d\Delta \left(m \frac{\Delta}{\varepsilon} \right)^2 e^{-\frac{\Delta^2}{2\varepsilon\hbar} m} e^{-\frac{i}{\hbar} \hat{p} \Delta} \right] e^{-\frac{\varepsilon}{2\hbar} V(\hat{x})}. \quad (2.32)$$

Substituting $\Delta' = \Delta + \frac{i\varepsilon}{\hbar} \hat{p}$ and performing the integration in eq. (2.32):

$$\sqrt{\frac{m}{2\pi\hbar\varepsilon}} \int d\Delta \left(m \frac{\Delta}{\varepsilon} \right)^2 e^{-\frac{\Delta^2}{2\varepsilon\hbar} m} e^{-\frac{i}{\hbar} \hat{p} \Delta} = \sqrt{\frac{m}{2\pi\hbar\varepsilon}} \int d\Delta' \left(\left(m \frac{\Delta'}{\varepsilon} \right)^2 - \hat{p}^2 \right) e^{-\frac{\Delta'^2}{2\varepsilon\hbar} m} e^{-\frac{\varepsilon}{2m\hbar} \hat{p}^2} = \left(\frac{\hbar}{\varepsilon} - \hat{p}^2 \right) e^{-\frac{\varepsilon}{2m\hbar} \hat{p}^2} \quad (2.33)$$

we find that the result diverges as $\frac{1}{\varepsilon}$. The final operator formula reads:

$$\left\langle \left(m \frac{x_{k+1} - x_k}{\varepsilon} \right)^2 \right\rangle = \frac{1}{Z_{N_T}} \text{Tr} \left(\hat{\mathcal{T}}^{N_T-k} \left(\frac{\hbar}{\varepsilon} - \hat{p}^2 \right) \hat{\mathcal{T}}^k \right). \quad (2.34)$$

The square of the momentum is an important observable, since it is proportional to the kinetic energy term in the Hamiltonian, however, the proposed form of functional (2.30) proves to be incorrect since results which are diverging as $\varepsilon \rightarrow 0$ are physically meaningless.

2.4. The point-splitting prescription

The point-splitting prescription is a way of defining a functional corresponding to the square of the momentum, which originates from the paper [5] of J. Schwinger. The following functional

$$p_{PS}^2 = m \frac{x_{k+1} - x_k}{\varepsilon} m \frac{x_k - x_{k-1}}{\varepsilon} \quad (2.35)$$

is considered as the new candidate for a quantity representing the square of momentum.

The path integral:

$$\langle p_{PS}^2 \rangle = \frac{1}{Z_{N_T}} \int \mathcal{D}x_{N_T}(t) \exp \left(-\frac{1}{\hbar} \varepsilon S[x_{N_T}(t)] \right) m \frac{x_{k+1} - x_k}{\varepsilon} m \frac{x_k - x_{k-1}}{\varepsilon}, \quad (2.36)$$

can be computed if it is decomposed as

$$\begin{aligned} \langle p_{PS}^2 \rangle = & \frac{1}{Z_{N_T}} \frac{m}{2\pi\hbar\varepsilon} \int \mathcal{D}x_{N_T-k-1}(t) dx_k dx_{k-1} \mathcal{D}x_{k-2}(t) \left(\prod_{i=k+1}^{N_T-1} \left(e^{-\frac{1}{\hbar}S(x_{i+1},x_i)} \right) e^{-\frac{1}{\hbar}S(x_{k+1},x_k)} m \frac{x_{k+1} - x_k}{\varepsilon} \right. \\ & \left. \times e^{-\frac{1}{\hbar}S(x_k,x_{k-1})} m \frac{x_k - x_{k-1}}{\varepsilon} \prod_{i=0}^{k-2} \left(e^{-\frac{1}{\hbar}S(x_{i+1},x_i)} \right) \right). \end{aligned} \quad (2.37)$$

Indeed, we already know that integration over $\mathcal{D}x_{k-2}(t)$ and $\mathcal{D}x_{N_T-k-2}(t)$ yields $\hat{\mathcal{T}}^{k-1}$ and $\hat{\mathcal{T}}^{N_T-k-1}$ respectively, whereas integration over dx_k and dx_{k-1} results in $\hat{\mathcal{T}} i\hat{p}$. Therefore, the appropriate operator formula reads:

$$\langle p_{PS}^2 \rangle = \frac{1}{Z_{N_T}} \text{Tr} \left(\hat{\mathcal{T}}^{N_T-k} i\hat{p} \hat{\mathcal{T}} i\hat{p} \hat{\mathcal{T}}^{k-1} \right). \quad (2.38)$$

Calculating the commutator:

$$\left[\hat{\mathcal{T}}, \hat{p} \right] = \left[e^{-\hat{H}\varepsilon + \mathcal{O}(\varepsilon^2)}, \hat{p} \right] = \frac{\hbar}{i} \frac{\varepsilon}{2} \left(e^{-\hat{H}\varepsilon + \mathcal{O}(\varepsilon^2)} V'(\hat{x}) + V'(\hat{x}) e^{-\hat{H}\varepsilon + \mathcal{O}(\varepsilon^2)} \right), \quad (2.39)$$

we finally arrive at the formula:

$$\langle p_{PS}^2 \rangle = \frac{1}{Z_{N_T}} \text{Tr} \left(\hat{\mathcal{T}}^{N_T-k} \left(-\hat{p}^2 + \mathcal{O}(\varepsilon) \right) \hat{\mathcal{T}}^k \right), \quad (2.40)$$

which, in the continuum limit, reads:

$$\langle p_{PS}^2 \rangle = \frac{1}{Z_T} \text{Tr} \left(e^{-\frac{1}{\hbar}\hat{H}(T-t_k)} \left(-\hat{p}^2 + \mathcal{O}(\varepsilon) \right) e^{-\frac{1}{\hbar}\hat{H}(t_k)} \right), \quad (2.41)$$

The minus sign in (2.41) originates from the transition to Euclidean time. Concluding, the point-splitting prescription (2.35) enables us to calculate the expectation value of the square of momentum.

3. Numerical evaluation of path integrals

3.1. Calculating path integrals using Monte Carlo methods

We are interested in computing the average value of a physical quantity represented by a functional $A[x_{N_T}(t)]$, therefore eq. (2.20) is the central point of our interest. The path integral in (2.20) can be simply viewed as a high-dimensional integral over the variables $x_0, x_1, \dots, x_{N_T-1}$. However, the integration can be performed analytically only in a few cases. Hence, a numerical method which works for an arbitrary potential $V(x)$ is employed.

A Monte Carlo method is used in order to calculate the path integral (2.20). Thus the task is to generate an ensemble of paths $x_{N_T}(t)$ so that the average value $\langle A \rangle$ is equal to the following limit:

$$\langle A \rangle = \frac{1}{Z_{N_T}} \int \mathcal{D}x_{N_T}(t) \exp\left(-\frac{1}{\hbar}S[x_{N_T}(t)]\right) A[x_{N_T}(t)] = \lim_{N_{sweep} \rightarrow \infty} \frac{1}{N_{sweep}} \sum_{i=1}^{N_{sweep}} A[x_{N_T}^i(t)], \quad (3.1)$$

where $x_{N_T}^i(t)$ is the i -th out of N_{sweep} generated paths. The equation (3.1) holds only if probability distribution in the ensemble of paths is given by:

$$\mathcal{P}[x_{N_T}(t)] = \frac{1}{Z_{N_T}} \exp\left(-\frac{1}{\hbar}S[x_{N_T}(t)]\right). \quad (3.2)$$

We will now address the question of generation of the ensemble of paths. In order to find paths that are distributed according to (3.2) we form a Markov chain of trajectories - we start with an initial trajectory $x_{N_T}^1(t)$ and generate subsequent paths $x_{N_T}^2(t), x_{N_T}^3(t), \dots, x_{N_T}^{N_{sweep}}(t)$. In the Markov chain the trajectory $x_{N_T}^i(t)$ is obtained from the previous one $x_{N_T}^{i-1}(t)$ according to a certain algorithm, such a process is characterized by $T[x'_{N_T}(t)|x_{N_T}(t)]$ - the probability of generating trajectory $x'_{N_T}(t)$ if starting from $x_{N_T}(t)$. Since $T[x'_{N_T}(t)|x_{N_T}(t)]$ is the transition probability, it satisfies the following requirements:

$$T[x'_{N_T}(t)|x_{N_T}(t)] \geq 0 \text{ and } \int \mathcal{D}x'_{N_T}(t) T[x'_{N_T}(t)|x_{N_T}(t)] = 1. \quad (3.3)$$

If, after k steps of the Markov process, probability distribution in the ensemble of paths is given by $P_k[x_{N_T}(t)]$, then it will be given by:

$$P_{k+1}[x'_{N_T}(t)] = \int \mathcal{D}x_{N_T}(t) T[x'_{N_T}(t)|x_{N_T}(t)] P_k[x_{N_T}(t)], \quad (3.4)$$

after another step of the Markov process.

Since our goal is to generate paths that are distributed according to (3.2), we impose the following requirement on the transition probability:

$$\frac{T[x'_{N_T}(t)|x_{N_T}(t)]}{T[x_{N_T}(t)|x'_{N_T}(t)]} = \frac{\mathcal{P}[x'_{N_T}(t)]}{\mathcal{P}[x_{N_T}(t)]}. \quad (3.5)$$

The condition (3.5) is known as the detailed balance condition and it is a sufficient condition for $\mathcal{P}[x_{N_T}(t)]$ to be an equilibrium distribution of the Markov process, because:

$$\int \mathcal{D}x_{N_T}(t) T[x'_{N_T}(t)|x_{N_T}(t)] \mathcal{P}[x_{N_T}(t)] = \mathcal{P}[x'_{N_T}(t)] \int \mathcal{D}x_{N_T}(t) T[x_{N_T}(t)|x'_{N_T}(t)] = \mathcal{P}[x'_{N_T}(t)]. \quad (3.6)$$

Having started from an arbitrary trajectory, after sufficiently large number of steps, the equilibrium distribution of the Markov process will be reached:

$$P_0 \xrightarrow{T} P_1 \xrightarrow{T} P_2 \xrightarrow{T} \dots \xrightarrow{T} \mathcal{P}. \quad (3.7)$$

Since we are interested in measuring $A[x_{N_T}(t)]$ on trajectories distributed according to (3.2) and the Markov chain was started from an arbitrary trajectory $x_{N_T}^1(t)$, the summation in (3.1) cannot include a certain number of initially generated trajectories. Therefore, a certain number of steps of the Markov process is performed and only when the equilibrium is reached and trajectories are being generated with probability (3.2) do we start to measure our observable. The process of approaching the equilibrium distribution is called the thermalization process.

3.2. The Metropolis algorithm

The Metropolis algorithm is an algorithm that performs one step of the Markov process considered in 3.1, i.e. it updates a trajectory $x_{N_T}^k(t)$ to obtain a new trajectory $x_{N_T}^{k+1}(t)$.

The trajectory $x_{N_T}^k(t)$, defined by the sequence of numbers (x_0, \dots, x_{N_T}) , is updated gradually, in one step of the algorithm only one value of x_j is modified, while the rest remains unchanged. The step of the algorithm is accomplished in the following way:

- A random number ξ is generated on interval $(-1, 1)$ with uniform probability density. Proposed new value of x_j is set as $x'_j = x_j + \xi\Delta$ where Δ is a fixed parameter. A trajectory $x_{N_T}'^k(t)$ defined by $(x_0, \dots, x_{j-1}, x'_j, x_{j+1}, \dots, x_{N_T})$ is examined.
- Difference between the values of actions for the trajectories $x_{N_T}'^k(t)$, $x_{N_T}^k(t)$:

$$\delta S = S[x_{N_T}'^k(t)] - S[x_{N_T}^k(t)] \quad (3.8)$$

is calculated and if $\delta S < 0$ then the trajectory $x_{N_T}'^k(t)$ is accepted.

- If $\delta S \geq 0$ then a random number r is generated with uniform distribution on the interval $(0, 1)$. The variable x_j is changed to x'_j if $e^{-\frac{1}{\hbar}\delta S} > r$. Otherwise, the previous value of the variable x_j is restored.

Afterwards, the algorithm proceeds to the next lattice site x_{j+1} . The procedure is repeated until all of the lattice sites (x_0, \dots, x_{N_T}) are probed and the new trajectory $x_{N_T}^{k+1}(t)$ is obtained.

Transition probability of a single update of x_j of the algorithm reads:

$$T_j[x_{N_T}'^k(t)|x_{N_T}^k(t)] = \min\left(1, e^{-\frac{1}{\hbar}\delta S}\right). \quad (3.9)$$

It is easy to see that:

$$T_j[x_{N_T}'^k(t)|x_{N_T}^k(t)]\mathcal{P}[x_{N_T}^k(t)] = \min\left(e^{-\frac{1}{\hbar}S[x_{N_T}^k(t)]}, e^{-\frac{1}{\hbar}S[x_{N_T}'^k(t)]}\right) = T_j[x_{N_T}^k(t)|x_{N_T}'^k(t)]\mathcal{P}[x_{N_T}'^k(t)], \quad (3.10)$$

thus the transition probability $T_j[x_{N_T}'^k(t)|x_{N_T}^k(t)]$ of one step of the algorithm fulfills the requirement (3.5) and as a result, the transition probability associated with the update of the whole trajectory $T[x_{N_T}^{k+1}(t)|x_{N_T}^k(t)]$ fulfills the detailed balance condition. Thus, once the thermalization process is completed, subsequent trajectories generated by the Metropolis algorithm are distributed according to (3.1).

Since in a single step of the Metropolis algorithm only one variable x_j is changed, the expression for δS (3.8) simplifies to:

$$\delta S = S[x_{N_T}'^k(t)] - S[x_{N_T}^k(t)] = \varepsilon \left(\left(\frac{x_{j+1} - x'_j}{\varepsilon} \right)^2 - \left(\frac{x'_j - x_{j-1}}{\varepsilon} \right)^2 + V(x'_j) - V(x_j) \right), \quad (3.11)$$

which means that computation of global values of action: $S[x_{N_T}'^k(t)]$ and $S[x_{N_T}^k(t)]$ in each step of the algorithm is unnecessary. It is sufficient to calculate δS according to (3.11). This simple observation considerably improves performance of the Metropolis algorithm.

3.3. Estimation of statistical errors

Having generated a set of N_{sweep} paths with the Monte Carlo algorithm, we are ready to start measuring $A[x_{N_T}(t)]$. Assuming that paths $x_{N_T}^1(t), \dots, x_{N_T}^{N_{therm}}(t)$ were generated before the thermalization process had been completed, whereas trajectories $x_{N_T}^{N_{therm}+1}(t), \dots, x_{N_T}^{N_{sweep}}(t)$ were generated by the algorithm in the equilibrium and thus are distributed according to (3.2), the following sequence of measurements is obtained:

$$(A[x_{N_T}^i(t)] : i = 1, \dots, x_{N_T}^{N_{therm}}, x_{N_T}^{N_{therm}+1}, \dots, x_{N_T}^{N_{sweep}}). \quad (3.12)$$

In order to find the average value $\langle A \rangle$ one may now compute the arithmetic average in (3.1). However, in numerical computations one deals with a finite N_{sweep} , hence the number of measurements $N_{meas} = N_{sweep} - N_{therm}$ is also finite, therefore verification of statistical errors plays a crucial role in analysis of Monte Carlo algorithms results.

Each value of $A[x_{N_T}^j(t)]$ ($j > N_{therm}$) in (3.12) corresponds to a random variable A^j . Since trajectories $x_{N_T}^j(t)$ were generated by the Markov process in equilibrium, all of these variables have the same expectation value and variance:

$$\overline{A^j} = \langle A \rangle \text{ and } \sigma_{A^j}^2 = \sigma_A^2, \quad (3.13)$$

where the overline denotes an average over a set of independent Markov chains. We use the unbiased estimators for these values from one Markov chain:

$$\check{A} = \frac{1}{N_{meas}} \sum_{i=N_{therm}+1}^{N_{sweep}} A^i \text{ and } \check{\sigma}_A^2 = \frac{1}{N_{meas} - 1} \sum_{i=N_{therm}+1}^{N_{sweep}} (A^i - \check{A})^2. \quad (3.14)$$

The estimator \check{A} is a random variable itself, as its value changes from one Markov chain to another. The variance of \check{A} is given by:

$$\sigma_{\check{A}}^2 = \overline{(\check{A} - \langle A \rangle)^2} = \frac{1}{N_{meas}^2} \sum_{i=N_{therm}+1}^{N_{sweep}} \overline{(A^i - \langle A \rangle)^2} + \frac{1}{N_{meas}^2} \sum_{\substack{i \neq j \\ i, j = N_{therm}+1}}^{N_{sweep}} \overline{(A^i - \langle A \rangle)(A^j - \langle A \rangle)}. \quad (3.15)$$

An important point is that in the case of trajectories generated with the Monte Carlo algorithm, the variables A^i, A^j are correlated since the successive trajectories $x_{N_T}^k(t), x_{N_T}^{k+1}(t)$ are obtained from each other. This leads to non-vanishing autocorrelation function, which, for a set Markov chains in equilibrium, is defined as:

$$C_A(t) = \overline{(A^k - \langle A \rangle)(A^{k+t} - \langle A \rangle)}. \quad (3.16)$$

Clearly, in order to calculate $C_A(t)$ in numerical computations, one does not average over the set of independent Markov chains, but rather uses an estimator from one Markov chain:

$$\check{C}_A(t) = \frac{1}{N_{meas} - t} \sum_{i=N_{therm}+1}^{N_{sweep}-t} (A^i - \check{A})(A^{i+t} - \check{A}). \quad (3.17)$$

Using the definition of $C_A(t)$ (3.16) one continues the calculation of $\sigma_{\check{A}}^2$ and according to [4] obtains:

$$\sigma_{\check{A}}^2 = 2 \left(\frac{1}{2} + \sum_{t=1}^{N_{meas}} \frac{C_A(t)}{C_A(0)} \right) \frac{1}{N_{meas}} \sigma_A^2 + \mathcal{O}\left(\frac{1}{N_{meas}^2}\right) \equiv 2\tau_{A,int} \frac{1}{N_{meas}} \sigma_A^2, \quad (3.18)$$

where the last equation defines integrated autocorrelation time $\tau_{A,int}$ and the term of order $\mathcal{O}(\frac{1}{N_{meas}^2})$ is dropped.

The equation (3.18) has two significant implications. The standard deviation of average value of A decreases with the number of measurements like $\frac{1}{\sqrt{N_{meas}}}$. Moreover, the statistical error (3.18) of the

result increases as the autocorrelations between generated trajectories become stronger. This can be interpreted in the following way: if the measurement was made on N_{meas} trajectories and the integrated autocorrelation time is estimated to be $\tau_{A,int}$, then the number of effectively independent measurements is:

$$N_{indep} = \frac{N_{meas}}{2\tau_{A,int}}. \quad (3.19)$$

Concluding, the resulting formula for the average value of the observable \hat{A} reads:

$$\langle A \rangle = \check{A} \pm \sqrt{2\tau_{A,int} \frac{1}{N_{meas}} \sigma_A^2}. \quad (3.20)$$

This equation shows the way of quoting results which will be adopted in section 4.

4. Results for harmonic oscillator

In this section we present results obtained with the Monte Carlo method introduced in the section 3 for harmonic oscillator. The method works for an arbitrary potential $V(x)$, we decide to choose the harmonic oscillator, since analytical solution of the problem is known and thus validity of our results can be easily verified.

The Hamiltonian of the harmonic oscillator reads:

$$\hat{H} = \frac{1}{2m}\hat{p}^2 + \frac{1}{2}m\omega^2\hat{x}^2, \quad (4.1)$$

where ω is the angular frequency.

4.1. Units and scales of the problem

Three dimensionful quantities appear in the Hamiltonian of harmonic oscillator:

$$[\hbar] = kg\,m^2\,s^{-1}, \quad [m] = kg, \quad [\omega] = s^{-1}. \quad (4.2)$$

The three quantities (4.2) determine the scale of the problem. Solving the physical problem with a computer demands defining dimensionless quantities, thus the three quantities (4.2) are combined in order to set units of mass, length, time, etc. and allow us to substitute dimensionful operators with dimensionless ones:

$$\hat{p} \rightarrow \frac{1}{\sqrt{m\omega\hbar}}\hat{p}, \quad \hat{x} \rightarrow \sqrt{\frac{m\omega}{\hbar}}\hat{x}, \quad \hat{H} \rightarrow \frac{1}{\hbar\omega}\hat{H}. \quad (4.3)$$

After this change any physical quantity becomes dimensionless, for instance, the average value of A (2.20) in the case of the harmonic oscillator potential reads:

$$\langle A \rangle = \frac{1}{Z_{N_T}} \int \mathcal{D}_{N_T} x(t) \exp \left(-\varepsilon \sum_{j=0}^{N-1} \left(\frac{1}{2} \frac{(x_{j+1} - x_j)^2}{\varepsilon^2} + \frac{1}{2} x_j^2 \right) \right) A[x_{N_T}(t)]. \quad (4.4)$$

Parameters which occur in our computer calculations split naturally into three groups:

- physical quantities: the mass m of the particle inside harmonic potential well, the angular frequency ω and the time T of evolution of the system. In units defined by (4.3) the mass and angular frequency are simply $m = 1$, $\omega = 1$ and we are left with only one physical parameter - the time T .
- parameter associated with the discretization of the trajectory - the number of time steps N_T , which is related to the size of a time step ε :

$$T = N_T \varepsilon. \quad (4.5)$$

- parameters of the Metropolis algorithm, among them the number of generated trajectories N_{sweep} is the most important, since it determines the statistical error of our results (3.20).

4.2. Thermalization, autocorrelation and critical slowing down

As pointed out in sec. 3.1, having started the Markov process of generation of paths from an arbitrary initial trajectory $x_{N_T}^1(t)$, we need to restrain ourselves from measurements until the thermalization process is completed, since only then the trajectories are generated according to the distribution (3.2).

We observe the process of thermalization of our algorithm by measuring value of certain x_j on subsequently generated trajectories, as function of number of generated paths - N_{sweep} , as presented in Figure 1. Figure 2 shows examples of trajectories generated during the process of thermalization and after the equilibrium was reached.

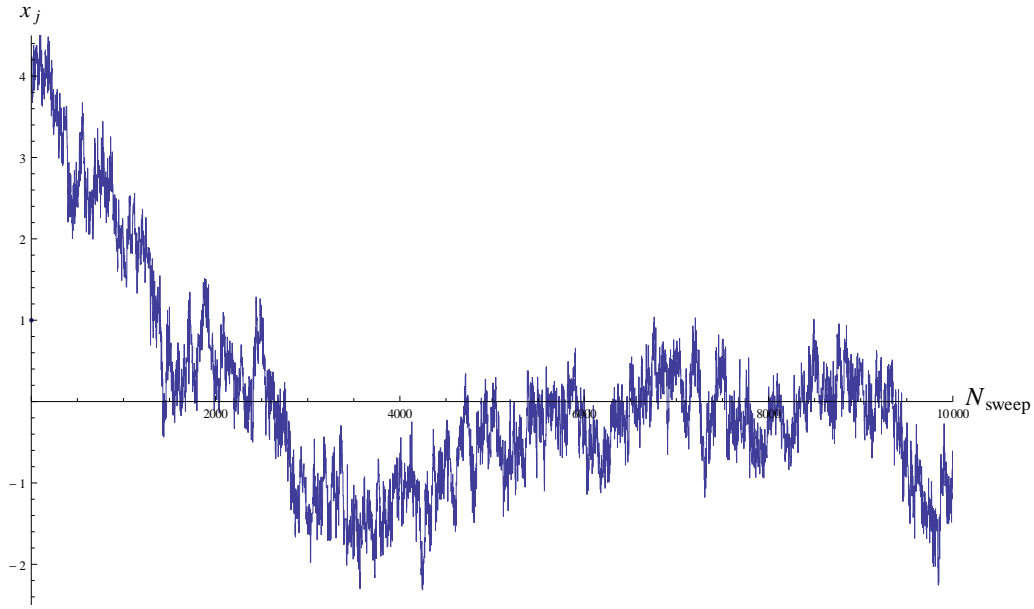


Figure 1: The value of x_j as function of N_{sweep} . The initial trajectory is $x_{N_T}^0(t) = \{4, \dots, 4\}$. This Figure illustrates the process of thermalization, we see clearly that the algorithm is approaching vicinity of paths with the value of x_j between -2 and 2 . In this case the thermalization process is finished when $N_{sweep} \approx 2000$. The parameters are $T = 2$, $N_T = 500$.

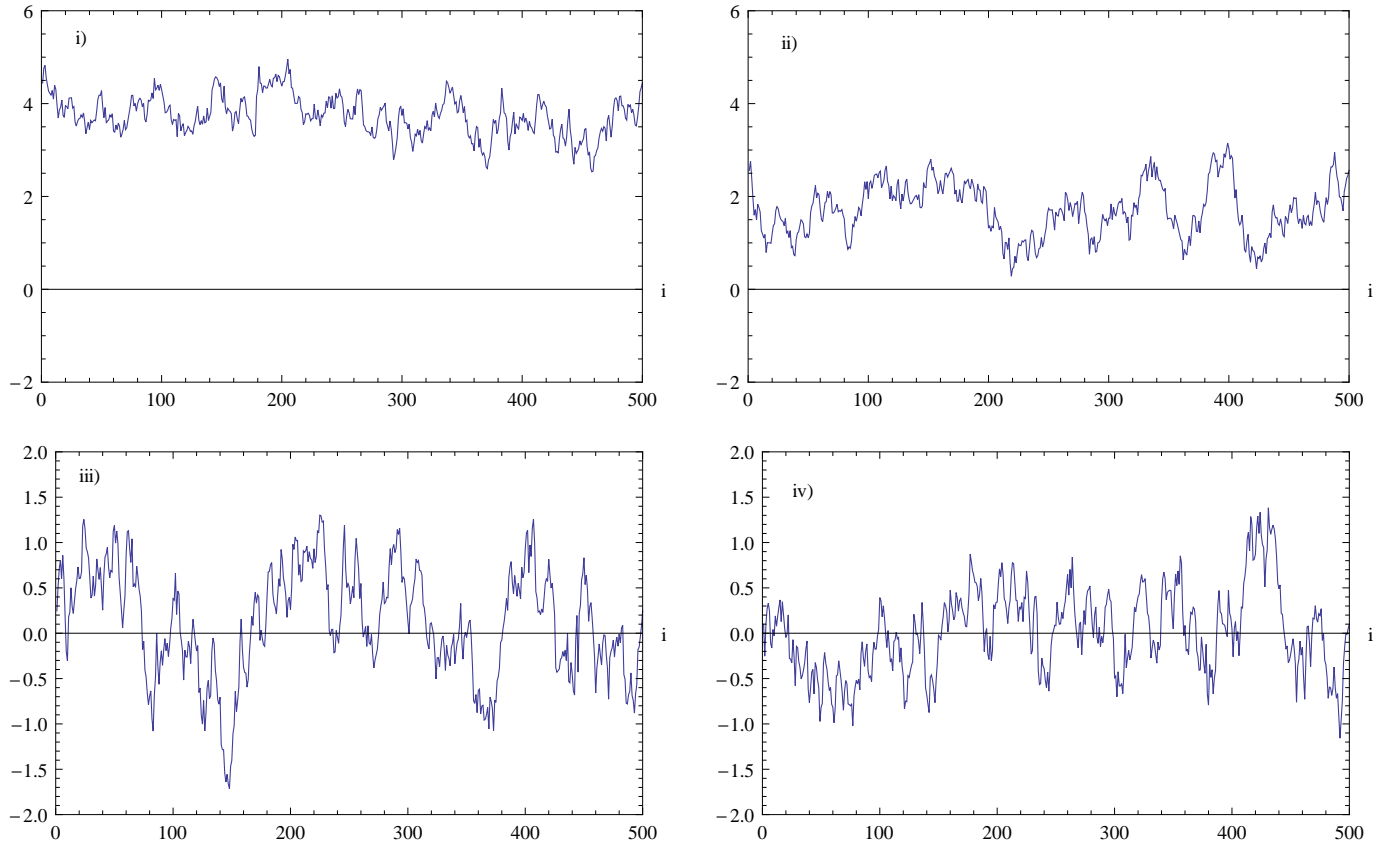


Figure 2: Paths, i.e. x_i as function of i , generated by the Metropolis algorithm during the process of thermalization presented on the Figure 1 for $N_{sweep} = 100$ –i), 1000 –ii), 5000 –iii), 20000 –iv). The trajectories i) and ii) are generated by the Markov process before reaching equilibrium - such trajectories occur with very small probability (3.2) in the Markov chain in the equilibrium and virtually do not contribute in measurements of observables. The trajectories iii) and iv) are generated by the Markov process in equilibrium and are typical trajectories of a quantum particle.

It is interesting to note that typical trajectories of a quantum particle presented in the Figure 2 are highly irregular, these paths resemble rather a random walk than a classical motion of the particle. This fact is in agreement with the equation (2.34) which tells us that no mean of the square of velocity exists at any point of the trajectory.

As pointed out in section 3.3, we expect that observables measured on subsequently generated trajectories will be autocorrelated. The integrated autocorrelation time $\tau_{A,int}$ for an observable \hat{A} defined by eq. (3.18) as:

$$\tau_{A,int} = \frac{1}{2} + \sum_{t=1}^{N_{sweep}} \frac{C_A(t)}{C_A(0)} \quad (4.6)$$

provides information on how strongly the subsequent measurements are correlated.

The autocorrelations are indeed observed in data obtained with the Metropolis algorithm. We investigate the autocorrelation of measurements of the position operator \hat{x} , Figure 3 shows $C_x(t)/C_x(0)$ as function of t .

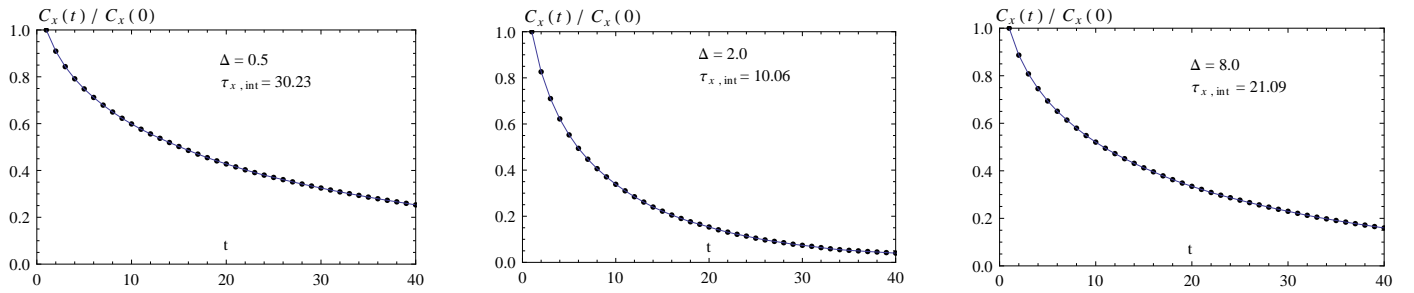


Figure 3: Plot presents $C_x(t)/C_x(0)$ as function of t i.e. the Monte Carlo time separation between subsequently generated paths. Parameters $T = 10$ and $N_T = 60$ are fixed, the Δ parameter which determines the maximum change of x_j in one step of the algorithm is set to 0.5, 2.0, 8.0. In order to minimize the statistical errors one has to minimize the data autocorrelation, which means that the Δ parameter must be carefully controlled during computations. Points are connected to guide the eye.

However, the major problem is the relationship between $\tau_{A,int}$ and N_T , since our aim is to perform calculation for possibly large N_T . Figure 4 shows $\tau_{x,int}$ as function of N_T .

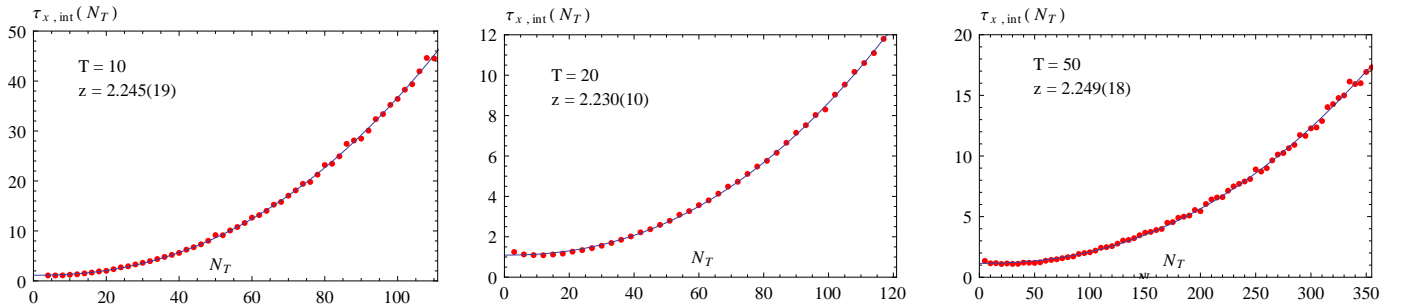


Figure 4: Plot presents $\tau_{x,int}$ as function of lattice size N_T for $T = 10, 20, 50$. We see that the autocorrelation time $\tau_{x,int}$ is increasing quickly with growing N_T . Function $f_T(N_T) = a(N_T)^z + b$ is fitted in each case, obtained exponents z are displayed on the plots.

We therefore observe that the integrated autocorrelation time $\tau_{x,int}$ varies as the z -th power of the lattice size N_T . The conclusion is that we observe a phenomenon known as the critical slowing down [4]. According to [4] $\tau_{A,int}$ is expected to behave as:

$$\tau_{A,int} \sim (N_T)^z \quad (4.7)$$

for any observable A . The important message of eq. (4.7) is that the numerical cost of obtaining results with relatively small statistical errors grows as z -th power of the lattice size N_T .

4.3. Fundamental observables \hat{x}^2, \hat{p}^2

In this section we are interested in average values of \hat{x}^2, \hat{p}^2 obtained with the Monte Carlo method.

The Monte Carlo method allows us to compute average values of observables according to eq. (2.20) for finite N_T , moreover, the value of N_T cannot be very large, since the computational effort grows as z -th power of N_T , according to eq. (4.7). Consequently, taking the limit $N_T \rightarrow \infty$, is not feasible. However, the continuum limit is part of the exact solution of a quantum mechanical problem with use of path integrals - cf. (2.6). Thus, the crucial question we have to address is how the fact, that we are restricted to study the system for relatively small values of N_T , influences our results.

The continuum limit cannot be performed on a computer, however, one can examine how the results depend on the value of N_T and expect, that if N_T is set to be large enough, the influence of time discretization will become negligible. Figure 5 shows computed values of the observables $\langle \hat{x}^2 \rangle, \langle p_{ps}^2 \rangle$ as functions of the lattice size N_T .

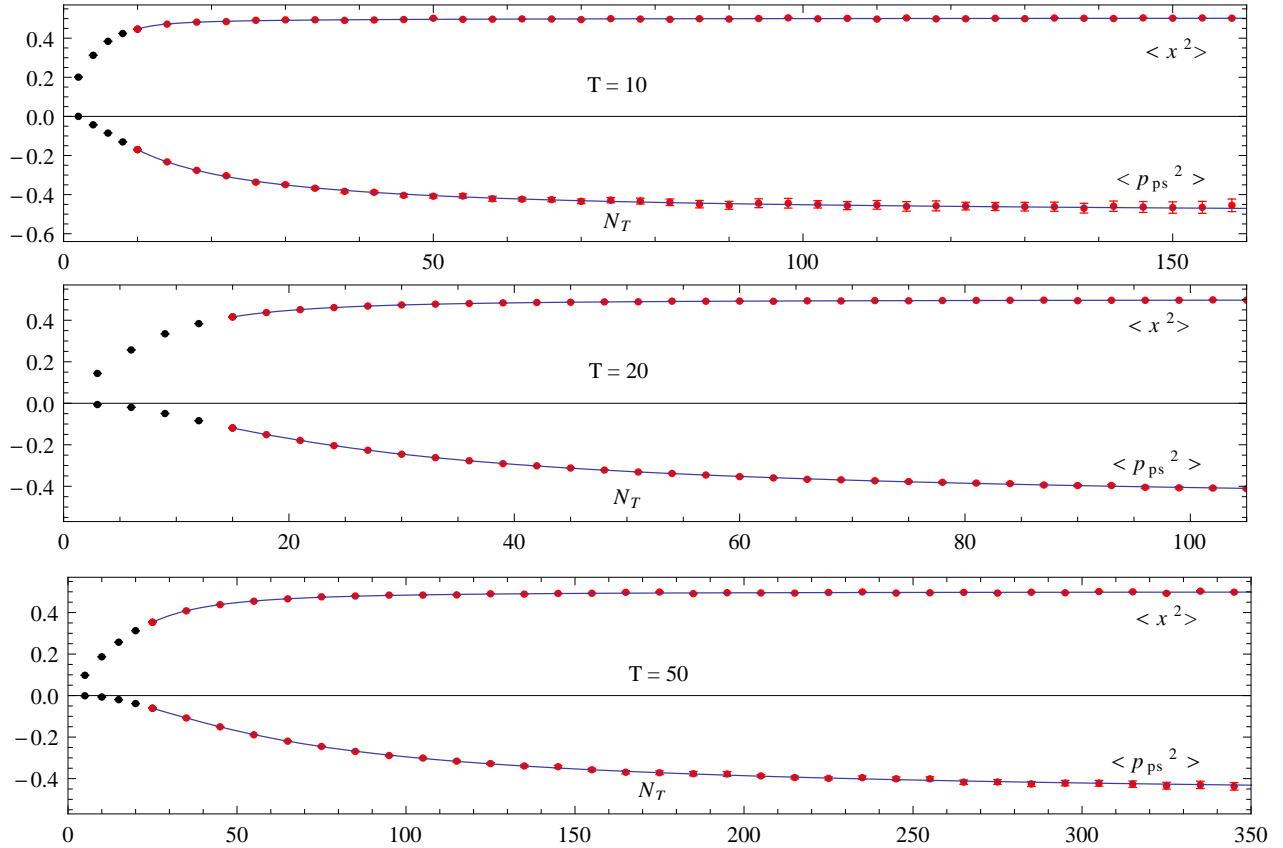


Figure 5: Mean values $\langle \hat{x}^2 \rangle, \langle p_{ps}^2 \rangle$ as functions of number of lattice sites N_T calculated for $T = 10, 20, 50$ and fitted functions $f_T(N_T)$.

Indeed, the values of $\langle \hat{x}^2 \rangle, \langle p_{ps}^2 \rangle$ are stabilizing with growing N_T . Fitting polynomials in $\frac{1}{N_T}$:

$$f_T(N_T) = \sum_{i=0}^3 P_i \left(\frac{1}{N_T} \right)^i, \quad (4.8)$$

where P_i are parameters of the fit, allows to extrapolate the Monte Carlo results to $N_T \rightarrow \infty$. Value of P_0 obtained in each fit approximates the continuum limit value:

$$\lim_{N_T \rightarrow \infty} \langle \hat{x}^2 \rangle \equiv \langle \hat{x}^2 \rangle_{CL}, \quad \text{and} \quad \lim_{N_T \rightarrow \infty} \langle p_{ps}^2 \rangle \equiv \langle p_{ps}^2 \rangle_{CL} \quad (4.9)$$

Obtained in this manner values of $\langle \hat{x}^2 \rangle_{CL}$ and $\langle p_{ps}^2 \rangle_{CL}$ are displayed in Table 1. We note, that results for $T = 20$ and $T = 50$ are in agreement within estimated statistical error and their absolute values are equal to $\frac{1}{2}$. We address the problem of meaning of the physical time T in the next section.

Table 1: Obtained values of $\langle \hat{x}^2 \rangle_{CL}$ and $\langle p_{ps}^2 \rangle_{CL}$

T	10	20	50
$\langle x^2 \rangle_{CL}$	0.50428(47)	0.49995(61)	0.50091(56)
$\langle p_{ps}^2 \rangle_{CL}$	-0.5034(69)	-0.4993(30)	-0.4994(31)

It follows from Figure 5 that p_{ps}^2 , as being more complicated functional than x^2 cf. 2.4, is converging more slowly to its continuum limit value than x^2 . Furthermore, we see that with growing T we need to set bigger and bigger values of N_T in order to be able to extract the continuum limit values of observables. It is interesting to confront this fact with Figure 4 which shows, that the constant a is decreasing as the value of N_T grows. Concluding, all the parameters in the problem are coupled and one has to put the same numerical effort to obtain physically significant results independently on value of T .

4.4. The ground state of the system

The time T of evolution of the system, the only physical parameter in the problem, plays an important role for it determines whether the higher energy states are present in our computations.

Calculating the average value of a local functional $A[x_{N_T}(t)] = A(x_k)$ in the basis of eigenstates $|n\rangle$ of the Hamiltonian \hat{H} we find:

$$\langle A \rangle = \frac{1}{Z_{N_T}} \text{Tr} \left(e^{-\hat{H}(T-t_k)} \hat{A} e^{-\hat{H}(t_k)} \right) = \frac{1}{Z_{N_T}} \sum_{n=0}^{\infty} \langle n | e^{-\hat{H}T} \hat{A} | n \rangle = \frac{1}{\sum_{n=0}^{\infty} e^{-E_n T}} \sum_{n=0}^{\infty} e^{-E_n T} \langle n | \hat{A} | n \rangle. \quad (4.10)$$

Eigenstates are ordered, $E_{n+1} < E_n$, thus:

$$\langle A \rangle \rightarrow \langle 0 | \hat{A} | 0 \rangle, \quad \text{for } T \rightarrow +\infty, \quad (4.11)$$

Therefore, calculation of $\langle A \rangle$ according to eq. (2.20) for sufficiently large T , provides the expected value of \hat{A} in the ground state of the system.

Let us now determine the value of T which is sufficient to separate the ground state of the system. Denoting the energy gap between n -th excited state and the ground state as: $\Delta_n = E_n - E_0$, we rewrite (4.10) in the following form:

$$\langle A \rangle = \frac{1}{\sum_{n=0}^{\infty} e^{-\Delta_n T}} \sum_{n=0}^{\infty} e^{-\Delta_n T} \langle n | \hat{A} | n \rangle, \quad (4.12)$$

The terms in the sums in eq. (4.11) are exponentially suppressed with growing Δ_n , thus, the larger the energy gaps Δ_n are, the lower value of T is sufficient to neglect the terms $e^{-\Delta_n T}$ with $n \geq 1$. We therefore see, that the difference between energies of the first excited state and the ground state - Δ_1 - determines the value of T which must be set in order to obtain the expectation value of the observable \hat{A} in the ground state of the system.

Exact value of Δ_1 is unknown, since E_1 and even E_0 are not determined yet. Hence, one cannot *a priori* tell which value of T is sufficient to isolate the ground state. We can, however, investigate how the value of time T influences the average value of certain observable \hat{A} and expect that $\langle A \rangle$ is stabilizing as T is growing larger.

The dependence of $\langle H \rangle$ on the value of T will be examined in this section. The functional which corresponds to the Hamiltonian \hat{H} (4.1) at time t_k reads:

$$H[x_{N_T}(t)] = -\frac{1}{2} \frac{(x_{k+1} - x_k)(x_k - x_{k-1})}{\varepsilon^2} + \frac{1}{2} x_k^2, \quad (4.13)$$

where $0 \leq k \leq N_T$ and the point splitting prescription (2.41) is used in the kinetic energy term. The minus sign in the kinetic energy term is an important detail, since it expresses the fact that we study evolution of the system in imaginary time - the i^2 appears in the second derivative $\frac{d^2 x(t)}{dt^2}$ (cf. section 2.4). In fact, the negative value of $\langle p_{PS}^2 \rangle$ has already been observed in section (4.3) and thus, the Hamiltonian H (4.13) is the sum of two quantities, both of which have the positive expectation value.

The Monte Carlo results are compared with the mean value of $\langle H \rangle$ calculated according to (4.10) i.e. $\langle H \rangle = \frac{1}{\sum_{n=0}^{\infty} e^{-E_n T}} \sum_{n=0}^{\infty} e^{-E_n T} E_n$, where the values of energies $E_n = \frac{1}{2} + n$ are obtained from the well known analytical solution of the time independent Schrödinger equation for the harmonic oscillator. The summation is performed analytically:

$$\langle H \rangle = \frac{1}{\sum_{n=0}^{\infty} e^{-(\frac{1}{2}+n)T}} \sum_{n=0}^{\infty} e^{-(\frac{1}{2}+n)T} (\frac{1}{2} + n) = -\frac{d}{dT} \text{Log} \left(\sum_{n=0}^{\infty} e^{-(\frac{1}{2}+n)T} \right) = \frac{1}{2} \text{Coth} \left(\frac{T}{2} \right). \quad (4.14)$$

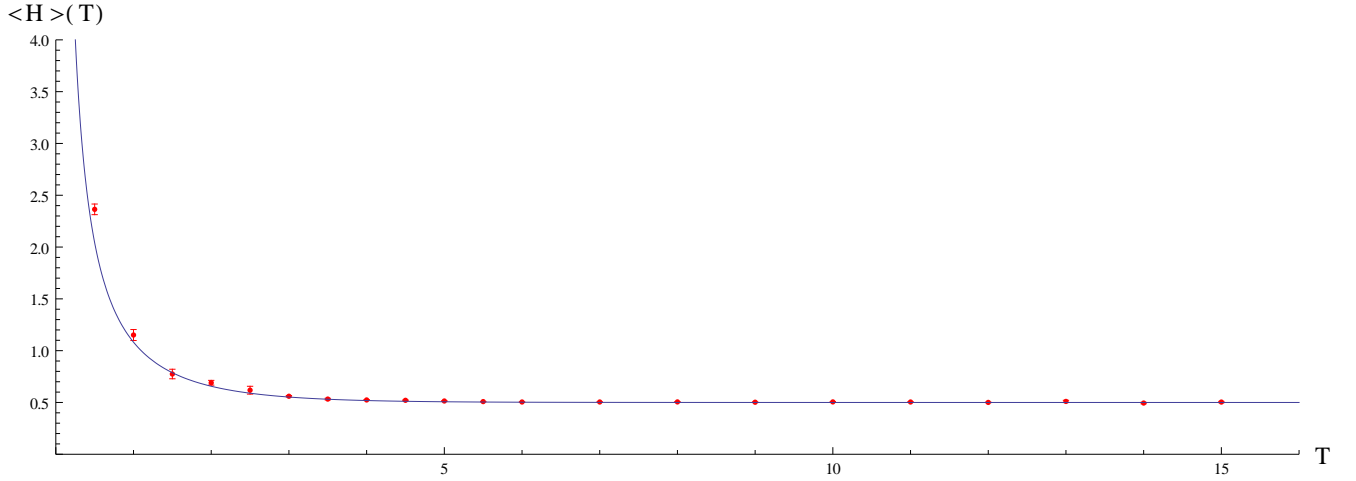


Figure 6: Mean value of the Hamiltonian $\langle \hat{H} \rangle$ (4.13) plotted as function of T . The red symbols denote results of our computations (every point represents the continuum limit value of $\langle \hat{H} \rangle$ for the corresponding time T). The function $\frac{1}{2} \text{Coth} \left(\frac{T}{2} \right)$ is plotted in blue.

Figure 6 presents $\langle H \rangle$ as function of T . The important message is that $\langle H \rangle$ is stabilizing as T is growing. Furthermore, the Figure 6 provides us with information about the value of T that is needed to be set in order to neglect the contribution of terms associated with higher energy states in (4.13). The sufficient value is approximately $T \approx 10$.

We are now able to interpret results presented in Table 1 and relate them with energy of the ground state of the system. The mean value of the kinetic energy in the ground state of the harmonic oscillator can be calculated according to the virial theorem as:

$$\langle 0 | \frac{1}{2} \hat{p}^2 | 0 \rangle = \langle 0 | \hat{x} \frac{dV(\hat{x})}{dx} | 0 \rangle = \langle 0 | \frac{1}{2} \hat{x}^2 | 0 \rangle, \quad (4.15)$$

which implies that the average value of the Hamiltonian is equal to:

$$\langle 0 | \hat{H} | 0 \rangle = \langle H \rangle = \langle x^2 \rangle = -\langle p_{PS}^2 \rangle, \quad (4.16)$$

for the sufficiently large T .

The energy of the ground state is equal to $E_0 = \frac{1}{2}$, which is known from the analytical solution of the harmonic oscillator. As pointed out in section 4.3 $\langle \hat{x}^2 \rangle_{CL}$ and $\langle p_{ps}^2 \rangle_{CL}$ for $T = 20$ and $T = 50$ are, within estimated statistical errors, equal to $\frac{1}{2}$ (or to $-\frac{1}{2}$ in case of $\langle p_{ps}^2 \rangle_{CL}$). The absolute values of $\langle \hat{x}^2 \rangle_{CL}$ and $\langle p_{ps}^2 \rangle_{CL}$ for $T = 10$ are slightly bigger than $\frac{1}{2}$ which means, that the contribution from the higher energy states is not entirely negligible for $T = 10$.

Concluding, the energy of the ground state of the harmonic oscillator is obtained and equal, as expected, to $\frac{1}{2}$. At this point the question about energies of the excited states can be addressed. Having generated results presented in Figure 6 and knowing the relationship between $\langle \hat{H} \rangle$ and T one could try to fit function such as:

$$f(T) = \frac{1}{\sum_{n=0}^{N_{cut}} e^{-P_n T}} \sum_{n=0}^{N_{cut}} e^{-P_n T} P_n, \quad (4.17)$$

to obtained results, where P_n would be parameters of fit, equal to sought energies E_n , and N_{cut} an arbitrary parameter. Unfortunately, such a method does not work properly even for $N_{cut} = 1$ - the fitted function is highly nonlinear and obtaining values of $\langle \hat{H} \rangle$ for small T with reasonable statistical errors requires a lot of numerical effort. The solution of problem of finding energies of higher energy states is presented in section 4.5.

4.5. Two-point correlation functions

4.5.1. Definition and relation to the higher energy states

Two-point correlation function (or simply two-point function) is a quantity which is evaluated from measurements of observables at two different times during evolution of system and therefore is dependent on the time separation t between the measurements. Two-point functions prove to be a convenient way in calculation of energies of excited states of a quantum system.

Let us consider the two-point correlation function of two local functionals $A_2[x_{N_T}(t)] = A_2(x_k) \equiv A_2(t_k)$ and $A_1[x_{N_T}(t)] = A_1(x_0) \equiv A_1(0)$:

$$\langle A_2(t_k) A_1(0) \rangle = \frac{1}{Z_{N_T}} \int \mathcal{D}x_{N_T}(t) e^{-S[x_{N_T}(t)]} A_2(t_k) A_1(0) = \frac{1}{Z_{N_T}} \text{Tr} \left(e^{-\hat{H}(T-t)} \hat{A}_2 e^{\hat{H}t} \hat{A}_1 \right). \quad (4.18)$$

The operator formula on the RHS of (4.18) can be obtained by a straightforward generalization of derivation of (2.25). Even though the order functionals $A_1(0)$ and $A_2(t_k)$ in the path integral (4.18) can be rearranged, the time succession of functionals (i.e. both are evaluated at different t) implies the structure of the operator formula.

The trace in (4.18), computed in the basis of eigenstates of the Hamiltonian, provides information about energies:

$$\langle A_2(t_k) A_1(0) \rangle = \frac{1}{Z_{N_T}} \sum_{n=0}^{\infty} \langle n | e^{-\hat{H}(T-t_k)} \hat{A}_2 e^{-\hat{H}t_k} \hat{A}_1 | n \rangle = \frac{1}{Z_{N_T}} \sum_{n,m=0}^{\infty} e^{-E_n T} e^{-(E_m - E_n)t_k} \langle n | \hat{A}_2 | m \rangle \langle m | \hat{A}_1 | n \rangle, \quad (4.19)$$

which becomes

$$\langle A_2(t_k) A_1(0) \rangle = \sum_{n=0}^{\infty} e^{-(E_n - E_0)t_k} \langle 0 | \hat{A}_2 | n \rangle \langle n | \hat{A}_1 | 0 \rangle \quad \text{for } T \rightarrow +\infty. \quad (4.20)$$

The energy gaps Δ_n are the only parameters in relationship between value of the two-point function and time t , provided that T is sufficiently large. Let us assume, that we are interested in the energy of the first excited state. If operators \hat{A}_1 and \hat{A}_2 , such that the matrix elements $\langle 0 | \hat{A}_2 | m \rangle$ and $\langle m | \hat{A}_1 | 0 \rangle$ are nonzero for $m = 1$ and are negligible for $m \neq 1$, were found, then we would be able to determine the value of Δ_1 , since one would expect a simple exponential dependence between the value of the two-point function and time t . Furthermore, we note that even if terms with $\langle 0 | \hat{A}_2 | m \rangle$ and $\langle m | \hat{A}_1 | 0 \rangle$ have to be taken into account for $m \neq 1$, the contribution of these terms becomes negligible for sufficiently large values of t , since $\Delta_m > \Delta_1$.

4.5.2. The first excited state of the harmonic oscillator

In this section the energy of the first excited state is determined. We consider a two-point function of $A_1[x_{N_T}(t)] = x_0$ and $A_2[x_{N_T}(t)] = x_k$. Such a choice of observables enables us to find the value of Δ_1 .

In our case, the two-point function, according to eq. (4.19), can be expressed as:

$$G_{\hat{x}}(t_k) \equiv \langle x_k x_0 \rangle = \frac{1}{Z_{N_T}} \sum_{n,m=0}^{\infty} e^{-E_n T} e^{-(E_m - E_n)t_k} |\langle m | \hat{x} | n \rangle|^2. \quad (4.21)$$

The operator \hat{x} enables us to determine the value of Δ_1 for the harmonic oscillator, since it is a linear combination of creation and annihilation operators:

$$\hat{x} = \frac{1}{\sqrt{2}} (\hat{a} + \hat{a}^\dagger), \quad (4.22)$$

where \hat{a} and \hat{a}^\dagger are defined in the standard way for the harmonic oscillator. Hence, the matrix element that appears in (4.21) is nonzero only if $m = n \pm 1$. If considered values of T are sufficiently large to isolate the ground state of the system, the two-point function becomes:

$$G_{\hat{x}}(t_k) = \sum_{n=0}^{\infty} e^{-(E_n - E_0)t_k} |\langle n | \hat{x} | 0 \rangle|^2 = e^{-(E_1 - E_0)t_k} |\langle 1 | \hat{x} | 0 \rangle|^2. \quad (4.23)$$

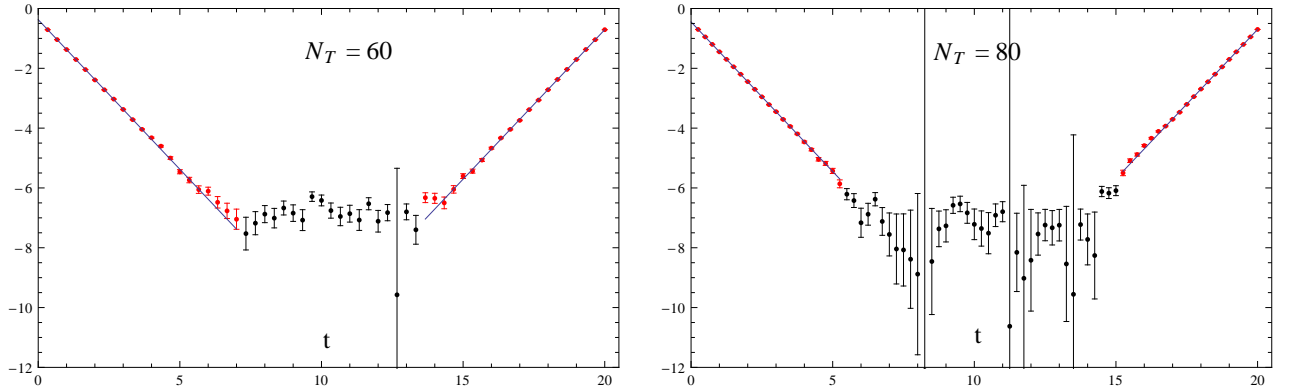


Figure 7: Plot presents $\text{Log}(\langle x_k x_0 \rangle)$ as function of t for $T = 20$ and different lattice sizes $N_T = 60, 80$. Fitted straight lines (4.24) are denoted in blue. We note that equation (4.21) is invariant under substitution $t \rightarrow T - t_k$, which results in the mirror symmetry of plots (up to denoted statistical errors).

Figure 7 presents the logarithm of $G_{\hat{x}}(t_k)$ as function of the time interval t_k . As expected, we observe that the value of two-point correlation function is exponentially suppressed as t_k grows. Therefore, functions $f_{N_T}(t)$:

$$f_{N_T}(t) = A e^{-\tilde{\Delta}_1 t}, \quad (4.24)$$

where $A, \tilde{\Delta}_1$ are parameters, are fitted to generated in the Monte Carlo simulation data and shown in the fig. 7. Resulting values of Δ_1 , equal to obtained values of $\tilde{\Delta}_1$, are displayed in Table 2.

We note that values of the first energy gap for $N_T = 60, 80, 100$ are, within estimated statistical errors, equal to 1. We claim that the slightly lower than 1 values of Δ_1 for $N_T = 20, 40$ are artifacts of the discretization of trajectories. Since values of Δ_1 for $N_T = 60, 80, 100$ are in agreement we conclude, that the continuum limit value of Δ_1 is a weighted arithmetic mean (with weights $\frac{1}{\sigma_{\Delta_1}^2}$) of results for $N_T = 60, 80, 100$:

$$\Delta_{1,CL} = 0.99847(59). \quad (4.25)$$

The value of $\Delta_{1,CL}$ is in agreement with the value known from the analytical solution i.e. 1, within 3 estimated standard deviations.

Table 2: Energy difference between first excited state and ground state ΔE_1 and its standard deviation σ_{Δ_1} for $T = 20$.

N_T	20	40	60	80	100
Δ_1	0.9678	0.99174	1.00043	0.9982	0.9956
σ_{Δ_1}	0.0079	0.00083	0.00093	0.0010	0.0012

4.5.3. The second excited state

We now proceed to find energy of the second excited state of the harmonic oscillator. According to (4.20), the value of Δ_2 can be computed similarly as Δ_1 in section 4.5.2, provided that we find operators \hat{A}_1 and \hat{A}_2 with vanishing matrix elements between the ground state and the first excited state: $\langle 1|\hat{A}_1|0\rangle$, $\langle 1|\hat{A}_2|0\rangle$.

A two-point correlation function of $A_1[x_{N_T}(t)] = x_k^2$ and $A_2[x_{N_T}(t)] = x_0^2$ is considered. The square of position operator \hat{x}^2 can be expressed as:

$$\hat{x}^2 = \frac{1}{2} (\hat{a}^2 + (\hat{a}^\dagger)^2 + 2\hat{a}^\dagger\hat{a} + 1), \quad (4.26)$$

with the aid of (4.22). The equation (4.26) means that the matrix element $\langle m|\hat{x}^2|n\rangle$ is nonzero only if $n = m \pm 2$ or $n = m$. Thus, in our case, the two-point function can be expressed as:

$$G_{\hat{x}^2}(t_k) = \langle x_k^2 x_0^2 \rangle = \sum_{n=0}^{\infty} e^{-(E_n - E_0)t_k} |\langle n|\hat{x}^2|0\rangle|^2 = |\langle 0|\hat{x}^2|0\rangle|^2 + e^{-(E_2 - E_0)t_k} |\langle 2|\hat{x}^2|0\rangle|^2 \quad (4.27)$$

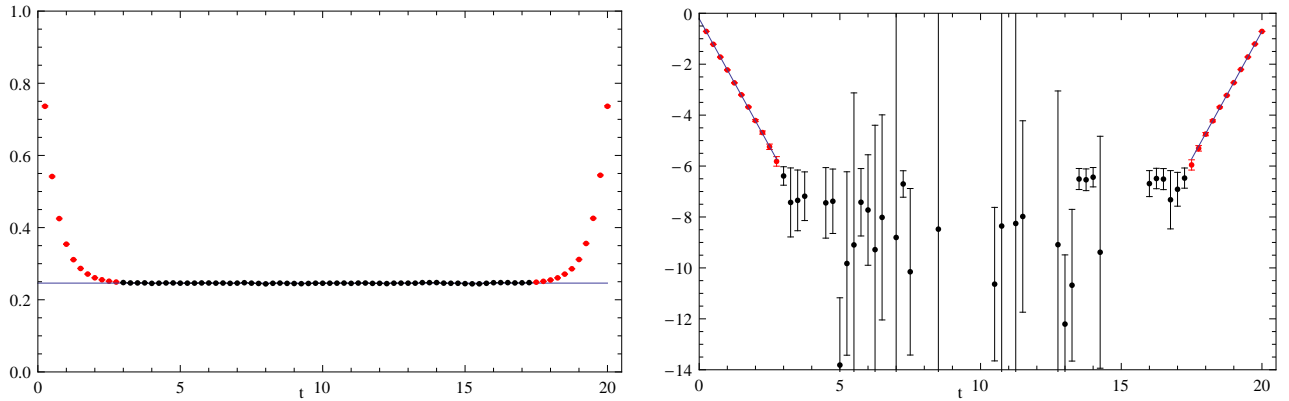


Figure 8: Plot on the left presents $\langle x_k^2 x_0^2 \rangle$ as function of t for $T = 20$ and $N_T = 80$. Plot on the right shows $\text{Log}(\langle x_k^2 x_0^2 \rangle - a)$, where a is constant function denoted as blue line on the left plot. The value of a is equal to square of the matrix element: $a = |\langle 0|\hat{x}^2|0\rangle|^2$, and as expected (cf. (4.26)) obtained values of a are, within statistical errors, equal to $\frac{1}{4}$.

Figure 8 presents computed values of the two-point propagator function of observable \hat{x}^2 . As expected, the two-point function, after subtraction of term which does not vanish as t becomes large, i.e. $\langle x_{t_k}^2 x_0^2 \rangle - |\langle 0|\hat{x}^2|0\rangle|^2$ depends exponentially on time t and therefore can be used in order to determine the value of Δ_2 . The value of Δ_2 is calculated similarly as Δ_1 in section 4.5.2 - exponential functions

$$f_{N_T}(t) = Ae^{-\tilde{\Delta}_2 t} \quad (4.28)$$

are fitted and displayed on the left plot of fig. 8. Parameters $\tilde{\Delta}_2$ obtained in fitting are equal to desired values of Δ_2 . Results are presented in Table 3.

Table 3: The second energy gap Δ_2 and its standard deviation σ_{Δ_2} calculated for $T = 20$.

L	20	40	60	80	100
Δ_2	1.9415	1.9883	2.0044	2.0056	1.9800
σ_{Δ_2}	0.0016	0.0051	0.0059	0.0067	0.0075

Again, we observe that results for $N_T = 60, 80, 100$ are in agreement within estimated statistical errors, while values of Δ_2 for $N_T = 20, 40$ are slightly lower. Calculating the continuum limit value of Δ_2 as the weighted arithmetic mean of results for $N_T = 60, 80, 100$, we obtain:

$$\Delta_{2,CL} = 1.9984(38). \quad (4.29)$$

The value of $\Delta_{2,CL}$ is in agreement with the value known from the analytical solution i.e. 2, within 1 estimated standard deviation.

5. Summary

In this thesis a way to tackle numerically quantum mechanical problems is presented. A self-contained description of the Monte Carlo method of evaluation of path integrals is introduced. It is employed in order to obtain energies of low lying states of one dimensional harmonic oscillator. Our work is characterized by an emphasis on practical and physical issues encountered in numerical calculation of path integrals which constitute common problems that have to be addressed in case of similar studies of more complex theories.

In the first part of this thesis we briefly introduced the path integral approach to quantum mechanics, which is equivalent to the operator technique. The fundamental correspondence between quantum mechanical operators and functionals evaluated for trajectories proved to be non-trivial and led us towards definition of the point-splitting prescription. To our knowledge, the derivation presented in sections 2.3 and 2.4 is novel. After the transition to the Euclidean time was performed, the factor which weights trajectories $e^{\frac{i}{\hbar}S[x_{N_T}(t)]}$ in the path integral became $e^{-\frac{1}{\hbar}S[x_{N_T}(t)]}$ and thus made the numerical calculation of path integrals feasible.

The next step was to note that the path integral, in the case of the time discretized trajectory, is a high dimensional integral over the lattice variables and as such can be evaluated with the Monte Carlo method. The Metropolis algorithm proved to be both feasible to implement and an efficient way of generating trajectories, however, in case of systems with a non-local action, performance of the Metropolis considerably decreases and one uses algorithms which base on different ideas - for instance the Hybrid Monte Carlo cf. [6].

Finally, having prepared the numerical method, we approached the problem of harmonic oscillator. We were rather interested in comprehension of the functioning of the Monte Carlo method than in obtaining excessively accurate results. The first step of analysis was to investigate the process of thermalization of the algorithm. It was found that measurements of the position observable on generated paths stabilize after a certain number of algorithm steps. Once the thermalization process was completed, we were able to measure physically interesting observables avoiding systematic errors. As one would expect, data obtained from measurements of an observable on subsequently generated trajectories were autocorrelated. These autocorrelations were growing stronger as the lattice size N_T was increasing, moreover, the integrated autocorrelation time turned out to be proportional to the power of the lattice size: $\tau_{A,int} \sim (N_T)^z$, which means that we encountered the critical slowing down of the algorithm. Then, the question of impact of the finite N_T on our results was addressed. Relationship between the mean values of observables \hat{x}^2 , \hat{p}^2 and the lattice size was examined, the resulting averages $\langle \hat{x}^2 \rangle$ and $\langle \hat{p}_{PS}^2 \rangle$ were found to be converging to their continuum limit values, which are of physical significance. The next step was to explore the dependence of time T of evolution of the system on our results. We have shown that the contribution of higher energy states in averages of observables is decreasing as T is becoming larger and that the value of T sufficient to isolate the ground state is determined by the first energy gap Δ_1 . Study of the expectation value of the Hamiltonian $\langle \hat{H} \rangle$ as function of T indicated, that $T \approx 10$ is enough to recover the average values in the ground state of the system. Eventually, the two-point correlation functions were defined and we found that the correlators of \hat{x} and \hat{x}^2 are convenient tool in determination of energies of the first and the second excited state of the system.

Concluding, this thesis demonstrates that path integrals can be effectively evaluated with use of Monte Carlo method. The main advantage of the method is its straightforward extension to systems with more degrees of freedom. A field theory is obtained when the time slicing is replaced by a space-time lattice. Furthermore, the method can be employed in investigation of non-perturbative problems, which play a crucial role in QCD. Hadron spectroscopy is an example of such a problem. Hadron masses can be obtained with use of the two-point function in the similar manner (cf. [2]) as energies of the first and the second excited states were obtained in this thesis.

Acknowledgements

I want to express my gratitude to my supervisor, Prof. Jacek Wosiek, for many useful discussions which deepened my understanding of path integrals and suggestions which helped to improve this manuscript.

Moreover, I would like to thank Andrzej Syrwid for the enjoyable time we spent in Zeuthen learning the path integral approach to quantum mechanics.

References

- [1] Feynman R.P., Hibbs A.R., *Quantum Mechanics and Path Integrals*, McGraw-Hill, New York 1965
- [2] Glattinger C., Lang C.B., *Quantum Chromodynamics on the Lattice*, Springer, Berlin Heidelberg 2010
- [3] Creutz M., Freedman B., *A Statistical Approach to Quantum Mechanics*, Ann. Phys. 132, 427-462 (1981)
- [4] Monvay I., Münster G., *Quantum Fields on a lattice*, Cambridge University Press, 1994
- [5] J. Schwinger, *On Gauge Invariance and Vacuum Polarization*, Phys. Rev. 82 (1951) 664
- [6] Sierant P., Syrwid A., *Path integral approach to simple quantum mechanical system*, Internal Report, Zeuthen 2012